SEISMIC PERFORMANCE OF PRECAST PC BEAMS USING SFRC

Hyeong Jae YOON, Ph.D., Engineer, TAISEI Corporation, Tokyo, Japan

ABSTRACT

Steel-Fiber Reinforced Concrete (hereafter referred to SFRC) is increasingly being used day by day as a structural material, for example, as coupling beam in coupled shear wall structures. Steel-fiber reinforced concrete is expected to enhance the tensile properties of the resulting composite such as strength and stiffness. Many researchers have proposed evaluation methods of the flexural strength and material model for steel-fiber reinforced concrete members in the past. In addition, only a few researches have been conducted to examine the role of fibers in the area of prestressed concrete applications. In this study, an attempt has been made to experimentally evaluate the seismic behavior of prestressed concrete beams using steel-fiber reinforced concrete. This study presents results from an experiment for two prestressed concrete beams and four prestressed concrete beams using steel-fiber reinforced concrete, where the main parameters were the volumetric ratios of steel-fibers: 0.0, 0.5 and 1.0 percent and the number of PC strands: 3 and 6. This research mainly attempted to evaluate the energy dissipation capacity and shear reinforcing effect of pre-tensioned beams using steel-fiber reinforced concrete. By using SFRC in PC beams, flexural strength was improved and the number of shear cracks was less than in beams without SFRC.

Keywords: Seismic Performance, Precast PC, Beam, SFRC

INTRODUCTIONS

In recent years, Steel-Fiber Reinforced Concrete material has been developed and studied for application to structural members such as coupling beams and seismic walls. A property of SFRC is the pseudo strain hardening behavior caused by the distribution of multiple fine cracks under tensile stress[1~3]. Steel-fibers have been used to enhance tensile characteristics of concrete by suppressing crack growth and improving mechanical behavior[4]. Concrete with steel-fibers is characterized by its steel-fiber content. The steel-fiber content is the weight of fibers per unit volume in concrete. It is the product of the volume fraction V_f (volume of fibers per unit volume of concrete, %) and the specific gravity of the fibers. It is still uncertain how the tensile characteristics of SFRC affect the flexural resistance mechanism of structural elements[2]. Various analytical and empirical methods have been proposed to predict the flexural strength of the composite material reinforced with fibers[5~7]. Of all the steel-fibers currently in use to reinforce cement matrices, steel-fibers are the only fibers that can be used for carrying long-term load[5, 8].

Prestressed concrete member requires the concrete to attain high compressive strength at an early stage to apply prestress force. In addition to its higher compressive strength, high strength concrete possesses an increased tensile strength and reduced shrinkage and creep strains than normal concrete. High strength concrete has been found, however, to be more brittle when compared to normal strength concrete. Inclusion of fibers is one way to alleviate the problem of brittleness in high strength concrete. Pretensioned concrete members have been used to control crack width and deflection under service load. Prestressing force applied on them is generally smaller than the one of post-tensioned members. However, construction cost of pretensioned members is lower than the one of posttensioned members because they do not need anchorage devices.

Table 1 summarizes the advantages and disadvantages of SFRC and prestressed members[7]. In order to overcome each disadvantage the synergy between SFRC and prestressing is expected to be one of the solutions under earthquake load. The present paper reports the influence of the steel-fiber reinforced concrete on the seismic behavior of prestressed concrete beam members under earthquake load.

EXPERIMENTAL PROGRAM

The main objective of this research was to evaluate the seismic behavior, energy

Table 1 Advantages and disadvantages of SFRC and prestressed member[7]

	Advantages	Disadvantages
SFRC	Smaller crack width enhancing durability More ductile	Constructability Cost
Prestressed member	Smaller residual deformation Smaller crack width	Brittle failure in compressed concrete

dissipation capacity and shear reinforcing effect of prestressed concrete beams using steel-fiber reinforced concrete (hereafter referred to PreSFC beam). The main variables in the test specimens were the volume fraction of steel-fibers; V_f=0.0, 0.5 and 1.0 percent and the number of PC strands located in each face; 3 (PC3 series) and 6 (PC 6 series).

Details of Specimens

The specimens are summarized in **Table 2** with the effective prestressing force P_e (kN) and the effective prestressing ratio η ($=P_e/(bDf'_c)$). The prestressing force P_e and the ratio η were calculated based on the strain measured immediately before loading by the strain gauges attached to the strands. Two traditional pretensioned beam (PC3: V_f=0.0%) and four pretensioned beams using SFRC (PC3-SF05: V_f=0.5%, PC3-SF10: V_f=1.0%) were constructed and tested under the reversed cyclic loading. All specimens were designed to fail in concrete crashing after tensile reinforcement yielded. The shear margin ratios (hereafter referred to $S.M.R.=Q_{su}/Q_{fu}$) of all specimens were about 1.19 as shown in **Table 2**. Q_{su} and Q_{fu} in **Table 2** are the ultimate shear strength and the shear force at the ultimate flexural strength calculated by Eq. (1) and (2) proposed by the *Design and calculation example of Prestressed Concrete Technical Standard*[9] (hereafter referred to Japan PC technical standard).

$$Q_{su}=b_0 \cdot j_0 \cdot p_w \cdot {}_wf_y+(b_0 \cdot D) \cdot (v \cdot F_c-2 \cdot p_w \cdot {}_wf_y)/2 \cdot \tan\theta \quad (1)$$

$$Q_{fu}=\{1-0.5(q+q_s)\} \cdot p \cdot b \cdot d^2 \cdot f_{py}+\{(d_s/d)-0.5(q+q_s)\} \cdot p_s \cdot b \cdot d^2 \cdot f_{sy} \quad (2)$$

in which b_0: width of cross section (mm), D: total depth of cross section (mm), j_0: distance from compression reinforcement to tensile steel (mm), F_c: compressive strength of concrete (N/mm^2), ${}_wf_y$: tensile strength of shear reinforcement (N/mm^2), p_w: shear reinforcement ratio, v: effective factors of concrete ($=\alpha L_f(1+\sigma'_g/F_c)$), $\alpha=(60/F_c)^{1/2}$,

Table 2 Steel-fiber contents, effective pre-stressing force and shear margin ratio

Specimen	V_f*1 (%)	P_e*2 (kN) (η*3)	Q_{su}*4 (kN)	Q_{fu}*5 (kN)	$S.M.R.$*6
PC3	0.0	433.3 (0.098)	513.0	420.0	1.22
PC3-SF05	0.5	457.0 (0.096)	533.0	424.0	1.26
PC3-SF10	1.0	386.1 (0.077)	509.0	427.0	1.19
PC6	0.0	512.6 (0.119)	462.0	402.0	1.15
PC6-SF05	0.5	651.7 (0.154)	466.0	398.0	1.17
PC6-SF10	1.0	609.8 (0.144)	455.0	399.0	1.14

*1: volume fraction of fibers, *2: effective prestressing force, *3: effective prestress ratio, *4: ultimate shear strength, *5: shear force at the ultimate flexural strength, *6: shear margin ratio, ($S.M.R.=Q_{su}/Q_{fu} \geqq 1.0$: flexural failure)

L_r=(M/(2Q ・ D)), σ'_g=P_e/(b_0D) (N/mm^2), q: factor of PC (=p_p ・ f_{py}/F_c), q_s: rebar factor of tensile rebar (=p_s・f_{sy}/F_c), p: ratio of PC strands (=A_p/(b・d)), A_p: area of PC strand (mm^2), p_s: rebar ratio of tensile rebar (=A_s/(b ・ d)), A_s: area of tensile rebar (mm^2), f_{py}: yield strength of PC strand (N/mm^2), f_{sy}: yield strength of tensile rebar (N/mm^2), b: width of section (mm), d: distance from compressive side of section to the center of PC strand (mm).

Fig. 1 shows the cross section of all the specimens. The cross section of all specimens was of the same size, 200 mm x 400 mm and the test section length was 1,110 mm, the total length was 2,500 mm as shown in **Fig. 1**. The prestressing tendons used in the test were 12.7 mm diameter strands. The prestressing force was introduced to the specimens one day after concrete casting. Thereafter, the specimens were removed from the pretensioning bed and moisture cured for 28 days. Japan PC Standard requires more than 45d for the development length of PC strand. In this study used 12.7 mm diameter strands, so the development length should be more than 571.5 mm. Size of the stub was decided by the size of the loading frame. Therefore, consideration of construction ability and size of stub, after assuring the required development length of PC strand 45d, the length of the beam end was 695 mm.

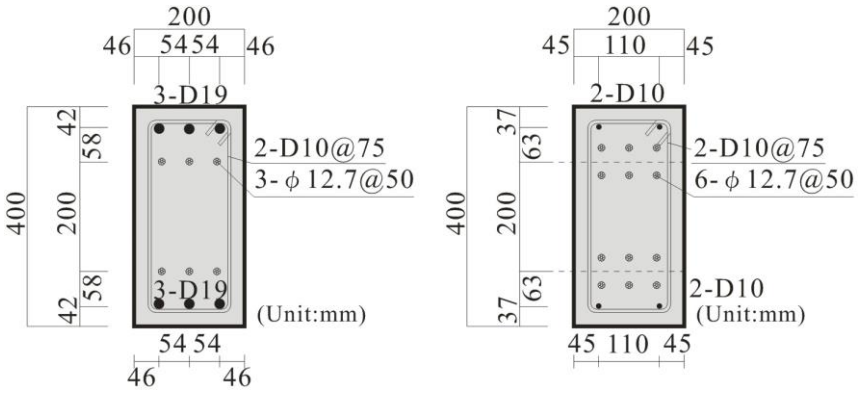

<PC3 series> <PC6 series>

(a) Section plan

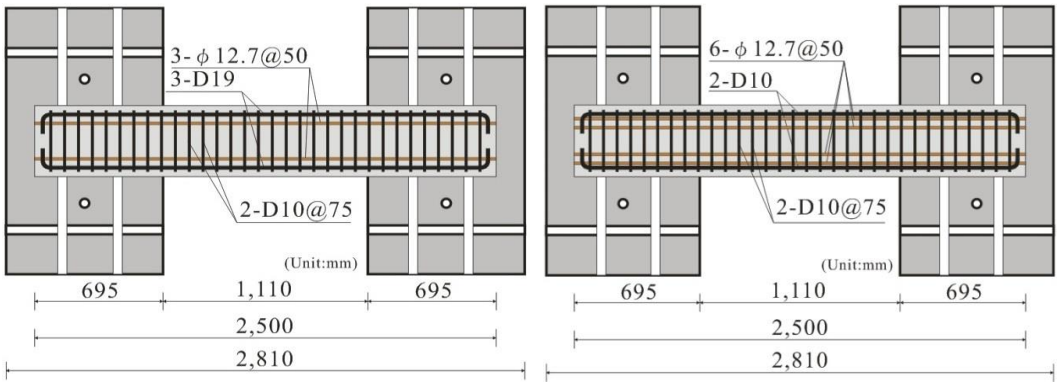

<PC3 series> <PC6 series>

(b) Reinforcements plan

Fig. 1 Details of specimens

Details of Materials

The base concrete mixtures were designed to give the compression strength of 60 N/mm^2 at 28 days. All specimens used an identical base concrete mixture as shown in **Table 3**. The water reducing agent content for SFC05 was 2.64 kg/m^3 and 3.01 kg/m^3 for SFC10. The test results of compressive and splitting tensile strengths at the time of testing are shown in **Table 4**. The compressive strength of the plain (V_f=0.0%) and steel-fiber reinforced concretes (V_f=0.5%, V_f=1.0%) varied from 55.1 to 62.5 N/mm^2. The splitting strength of the plain concrete was 3.44 N/mm^2 while the one of SFRC concretes were 3.51 and 4.53 N/mm^2.

Fig. 2 and **Fig. 3** show the stress-strain relationships in compression and splitting tensile tests. The average strain in splitting tensile was measured by a 60 mm wire strain gauge attached horizontally across a vertical crack. The compressive strain at the compressive strength of normal concrete (hereafter referred to NC, V_f=0.0%), SFC05 (V_f=0.5%) and SFC10 (V_f=1.0%) were 0.229, 0.268 and 0.283 percent, respectively.
The strain at the peak splitting tensile strength of NC was 0.017 percent while SFC05 and SFC10 were 0.017 and 0.025 percent. NC lost the strength immediately after it reached the strength in the compressive and splitting tensile test results as shown in **Fig. 2** and **3**.

Table 5 shows the material test results of the reinforcing bars and the prestressing strands used in this study. The average yield strengths of D10 and D19 bars were 498 and 537 N/mm^2 and the young's modulus were 1.98x10^5 and 2.01x10^5 N/mm^2, respectively.

Table 3 Design of concrete mix proportion

Type	Design strength (N/mm^2)	V_f (%)	Slump (cm)	W/C (%)	Air (%)	Water (kg/m^3)	Cement (kg/m^3)
NC	60	0.0	15.0	42.0	4.5	158	376
SFC05		0.5					
SFC10		1.0					

Type	Design strength (N/mm^2)	V_f (%)	Aggregate (kg/m^3)		Admixture (kg/m^3)	
			S*1	G*2	W.R.A*3	A.E.A*4
NC	60	0.0	808	951	2.44	0.75
SFC05		0.5			2.63	0.00
SFC10		1.0			3.01	

*1: fine aggregate, *2: coarse aggregate, *3: water reducing agent, *4: air entraining agent

Table 4 Concrete Properties

Specimens	Con'c Type	Compressive strength, f'_c (N/mm^2)	Strain at compressive strength (%)	Splitting tensile strength, f_{sp} (N/mm^2)	Modulus of elasticity at 1/3f'_c, E_c (x10^{4}N/mm^2)	Poisson's ratio
PC3	NC	55.1	0.259	3.44	3.17	0.193
PC3-SF05	SFC05	59.3	0.268	3.51	3.47	0.202
PC3-SF10	SFC10	62.5	0.283	4.53	3.68	0.249
PC6	NC	53.8	0.030	3.02	3.15	0.175
PC6-SF05	SFC05	52.9	0.035	2.73	2.86	0.181
PC6-SF10	SFC10	53.0	0.037	2.75	2.69	0.195

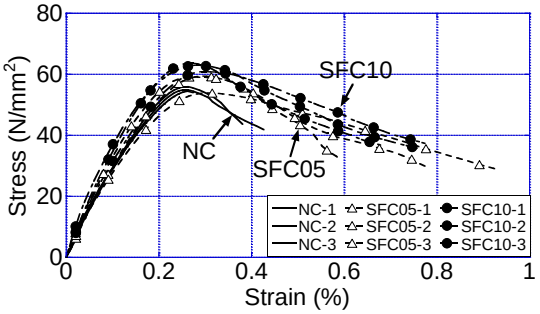

Fig. 2 Compressive stress-strain

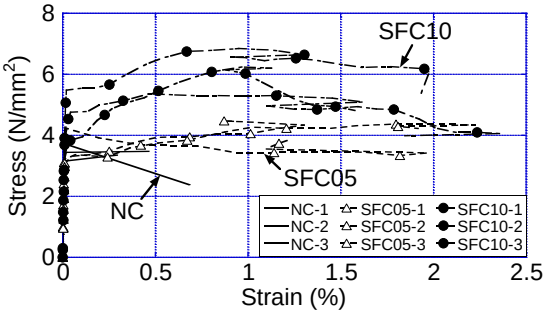

Fig. 3 Splitting tensile stress-strain

Table 5 Properties of reinforcing bars and prestressing strand

Reinforcement	Yielding strength (N/mm^2)	Tensile strength (N/mm^2)	Young's modulus (x10^5 N/mm^2)
D10(SD295)	376	498	1.98
D19(SD345)	358	537	2.01
ϕ 12.7(SWPR7BL)	1,798	1,980	2.02

Table 6 Properties of steel-fiber

Dimension (mm x mm)	Tensile strength (N/mm^2)	Young's modulus (N/mm^2)	Specific gravity	Aspect ratio
Φ0.62 x 30	1,050	206,000	7.85	48.4

Table 7 Reinforcement ratio at balanced failure

Specimen	Reinforcement ratio by cross section (%)	Reinforcement ratio at balanced failure (%)
PC3	1.69	2.35
PC3-SF05		2.52
PC3-SF10		2.68
PC6	1.18	1.51
PC6-SF05		1.51
PC6-SF10		1.51

Reinforcing bars used were D10 for the stirrups and D19 for the longitudinal bars of all specimens. All the specimens had the same longitudinal rebar ratio of 1.2 percent and the shear reinforcement ratio of 0.95 percent. The properties of steel fibers are summarized in **Table 6**.

Table 7 shows the reinforcement ratio at balanced failure of all specimens. PC3 and PC6 series specimens had longitudinal steel ratio of 1.63 and 1.18 percent. The reinforcement ratio at balanced failure of PC3, PC3-SF05 and PC3-SF10 were 2.35, 2.52 and 2.68 percent, respectively. PC6, PC6-SF05 and PC6-SF10 had the same reinforcement ratio at balanced failure of 1.51 percent, respectively. Therefore, all the specimens were expected to enhance the flexural strength by steel-fibers.

Loading Setup and Location of LVDTs, Strain Gauges

The loading setup is illustrated in **Fig. 4**. To simulate a beam in the moment-resisting frame subjected to earthquake loading, the vertical jacks of 8,000kN capacity kept the top stub horizontal during testing. The total load of these two oil-jacks was continually kept to zero so that no axial load was applied on the beam.

The first loading cycle was up to drift angle R=0.05 percent, and was followed by a series of member rotation controlled cycles comprising two full cycles to each of the member rotation of 0.1, 0.25, 0.5, 0.75, 1.0, 2.0, 3.0, 4.0 and 5.0 percent. **Fig. 5** shows the location of displacement transducers (LVDT) and wire strain gauges on the reinforcement.

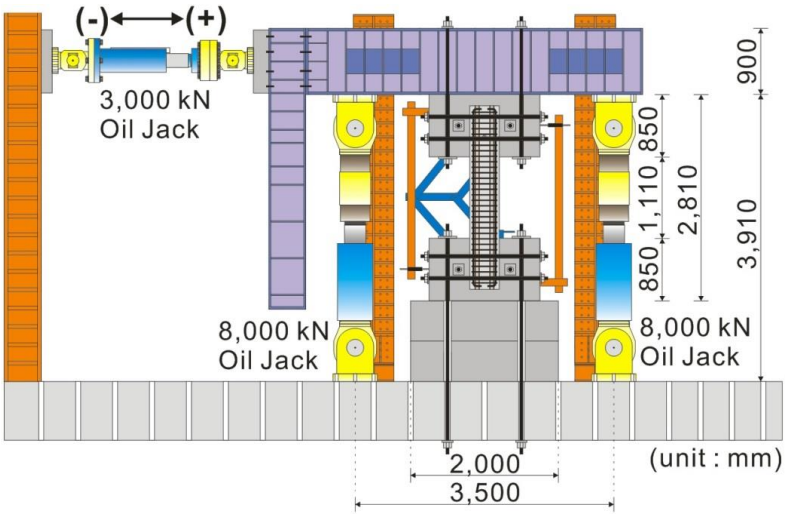

Fig. 4 Loading setup

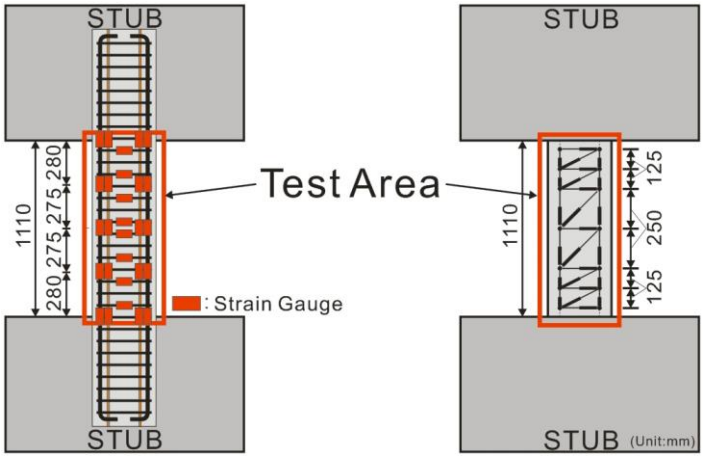

Fig. 5 Locations of LVDTs and strain gauges

TEST RESULTS

Shear Force-Drift Angle Relationships

Fig. 6 shows the shear force-drift angle curves for all specimens. The $Q_{cal.}$ in the graphs is the design maximum strength calculated by the Japan PC technical standard[9] as shown Eq. (2).

Fig. 7 shows the stress-strain distribution in PC member used in this study. The current Japan PC technical standard does not have a strength calculation method for members using steel-fiber reinforced concrete. The effect of fiber reinforcement was not taken into account for the calculation of $Q_{cal.}$.

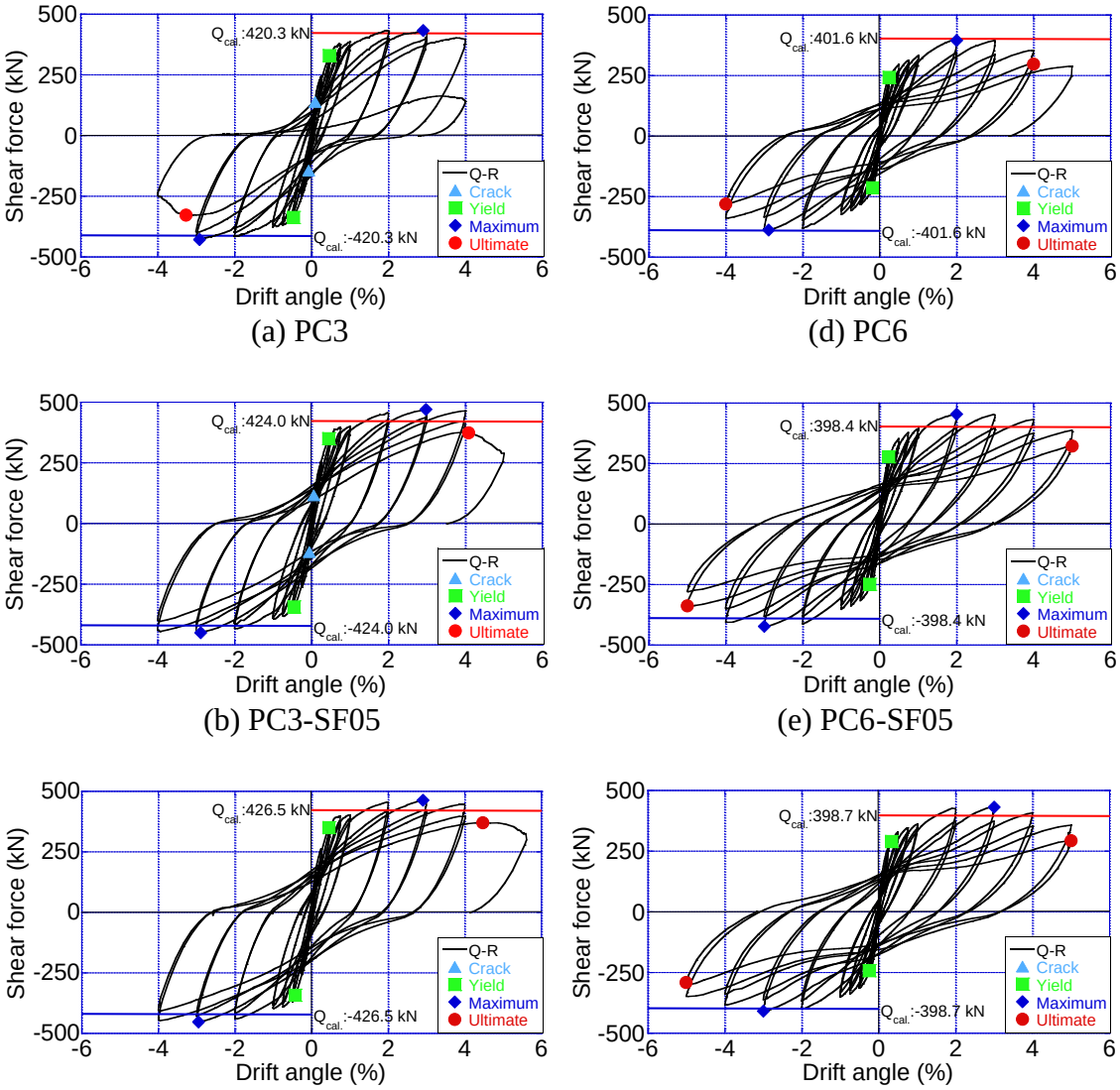

(a) PC3 (d) PC6

(b) PC3-SF05 (e) PC6-SF05

(c) PC3-SF10 (f) PC6-SF10

Fig. 6 Shear force-drift angle curves

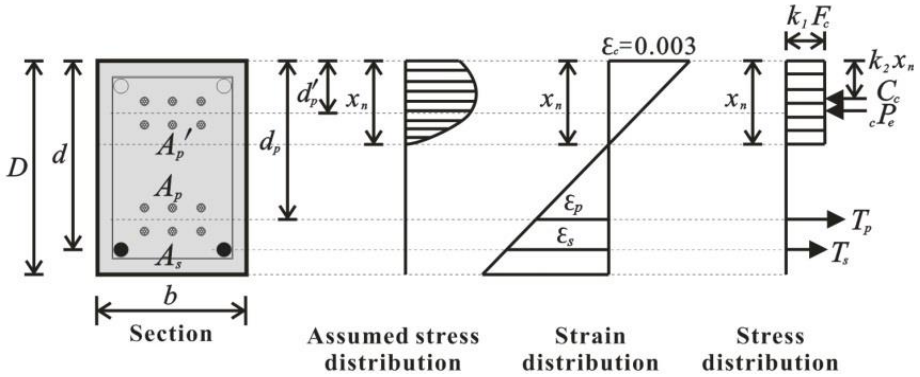

Fig. 7 Stress-strain distribution in PC members

Table 8 summarizes the test results for all specimens;
Yield: the measured strains of longitudinal mild steel rebar reached the yield strains.
Maximum: the maximum load was attained.
Ultimate: the load reduced to 80 percent of the maximum load.

The initial prestressing plan and concrete mix proportion of PC3 series and PC6 series were similar. However, the cover concrete was a little different, PC3 and PC6 were 42 mm and 37 mm. Moreover, the concrete strengths of PC6 series were smaller than PC3 series although the same concrete mix proportion was used. As a result, the first crack strengths of PC6 series specimens were smaller than PC3 series as shown in Table 8(1).The maximum strengths of PC3 and PC6 were almost the same as the calculated strength as shown in **Fig. 6** (a) and (d), while PC3-SF05, PC3-SF10, PC6-SF05 and PC6-SF10 specimens were higher than the design strength varied from 2.5 to 14.0

Table 8(1) Summary of test results

Specimens	First cracking				Yield[*1]			
	(+)		(-)		(+)		(-)	
	Q_{cr} (kN)	R_{cr} (%)	Q_{cr} (kN)	R_{cr} (%)	Q_y (kN)	R_y (%)	Q_y (kN)	R_y (%)
PC3	138.0	0.092	144.4	0.073	329.2	0.460	337.3	0.467
PC3-SF05	115.8	0.057	118.1	0.058	349.7	0.447	343.9	0.455
PC3-SF10	139.6	0.078	129.6	0.075	350.4	0.450	342.0	0.428
PC6	105.6	0.056	108.0	0.056	242.8	0.245	214.1	0.180
PC6-SF05	115.0	0.055	109.4	0.051	278.0	0.235	249.1	0.255
PC6-SF10	111.7	0.054	110.3	0.057	289.7	0.332	242.6	0.246

Table 8(2) Summary of test results

Specimens	Maximum[*2]				Ultimate[*3]			
	(+)		(-)		(+)		(-)	
	Q_{max} (kN)	R_{max} (%)	Q_{max} (kN)	R_{max} (%)	$Q_{ult.}$ (kN)	$R_{ult.}$ (%)	$Q_{ult.}$ (kN)	$R_{ult.}$ (%)
PC3	432.9	2.903	428.6	2.911	-	-	327.6	3.261
PC3-SF05	470.3	2.974	450.2	2.881	373.7	4.086	-	-
PC3-SF10	462.9	2.909	452.9	2.951	370.3	4.470	-	-
PC6	395.6	2.003	388.4	2.885	297.6	4.001	280.8	3.997
PC6-SF05	454.2	1.999	422.8	2.995	322.6	5.000	337.9	5.000
PC6-SF10	431.3	3.001	408.6	2.999	293.3	5.002	290.7	5.009

*1: at the yield of rebar, *2: at peak load, *3: at the load reduced to 80% of Q_{max}

Table 9 Comparison of maximum strength

Specimens	Test (kN)		Eq.(2)*1 (kN)	Test / Eq.(2) (%)	
	(+)	(-)		(+)	(-)
PC3	432.9	428.6	420.3	103.0	102.0
PC3-SF05	470.3	450.2	424.0	110.9	106.2
PC3-SF10	462.9	452.9	426.5	108.5	106.2
PC6	395.6	388.4	401.6	98.5	96.7
PC6-SF05	454.2	422.8	398.4	114.0	106.1
PC6-SF10	431.3	408.6	398.7	108.2	102.5

*1: maximum strength by Japan PC standard, Eq. (2)

percent as shown in **Table 9**. Because the Japan PC technical standard does not consider the effect of fiber reinforcement, this was not taken into account for the calculation of $Q_{cal.}$. Therefore, the strength improvement effect of pretensioned members was confirmed due to the use of steel-fiber reinforced concrete.

Cracking and Crushing Behaviors

Fig. 8 and **Fig. 9** show the cracking and failure pattern at end of testing for all specimens. The numbers of shear cracks of PC3 and PC6 specimens were more pronounced than the other specimens: PC3-SF05, PC3-SF10, PC6-SF05 and PC6-SF10. All specimens failed due to concrete crushing at the end of test area as shown in **Fig. 8** and **9**.

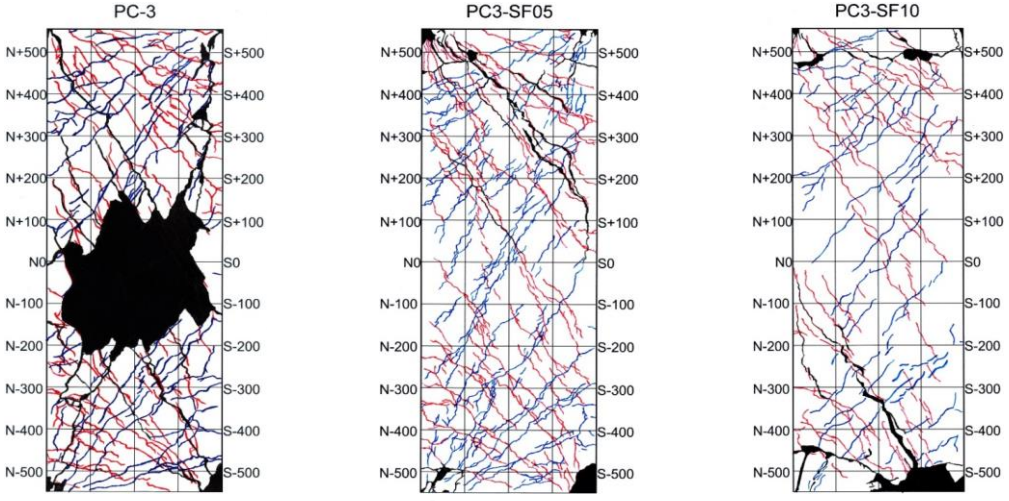

(a) PC3 (b) PC3-SF05 (c) PC3-SF10

Fig. 8 Cracking and failure pattern after testing: PC3 series

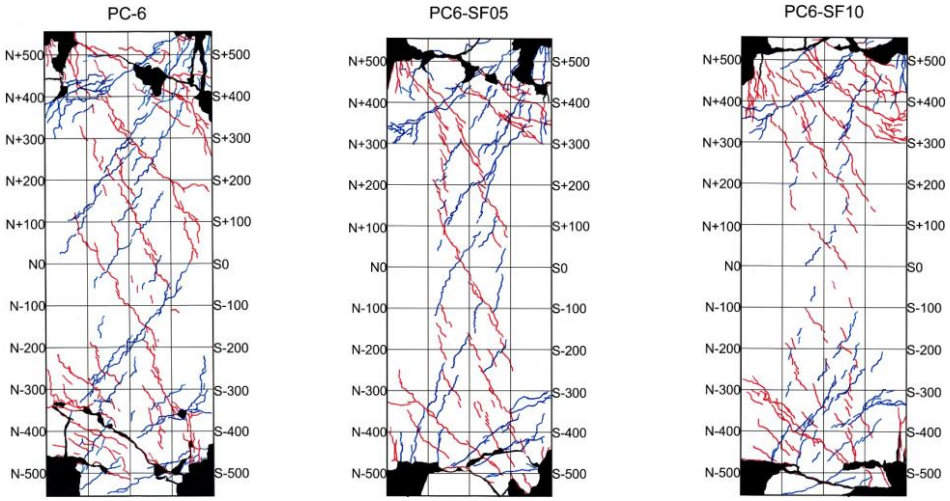

(a) PC6 (b) PC6-SF05 (c) PC6-SF10

Fig. 9 Cracking and failure pattern after testing: PC6 series

The first flexural crack in all specimens occurred at both end regions of test area. Specimen PC3 showed permanent damage since the cover concrete had spalled off and the prestressing strands and mild reinforcement were exposed. However, for PC3-SF05 and PC3-SF10, the concrete spalling did not occur as shown in **Fig. 8(b)** and **(c)**. In addition, it can be seen for PC3-SF10 that the number of shear cracks was less than that for PC3 and PC3-SF05. However, PC6 specimen did not show cover concrete spalling like for PC3 specimen while the compressive failure at the end was more severe than that for PC3 as shown in **Fig. 9(a)**. This is because the amount of PC strands for PC6 specimen was 2 times more than that for PC3 specimen. Moreover, it can be seen for PC6-SF05 and PC6-SF10 that the number of shear cracks was less than that for PC6 specimen. This is because there was a shear reinforcing effect by steel-fiber reinforced concrete.

DISCUSSIONS

Energy Dissipation Capacity

One of the objectives of this research was to evaluate whether integrating ductile steel-fiber reinforced concrete into pretensioned beams increases energy dissipation over traditional pretensioned beam. The energy dissipation capacity for each specimen, h_{eq} (equivalent viscous damping), was estimated by calculating the area enclosed by the hysteretic loops for each cycle of each specimen as given by Eq. (3) and as shown in **Fig. 10**.

$$h_{eq}=1/(4\pi)\cdot(\Delta A/(A_1+A_2))\ \text{x}\ 100\ (\%) \quad (3)$$

in which ΔA: area of loop, A_1 and A_2: area of triangle OAB and OCD as shown in **Fig. 10**.

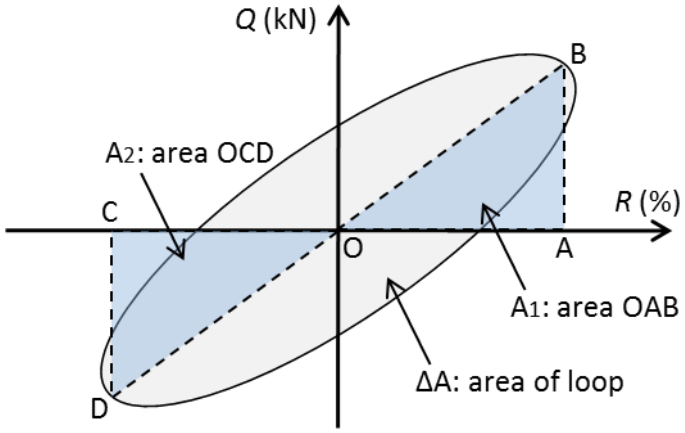

Fig. 10 Concept of h_{eq} calculation

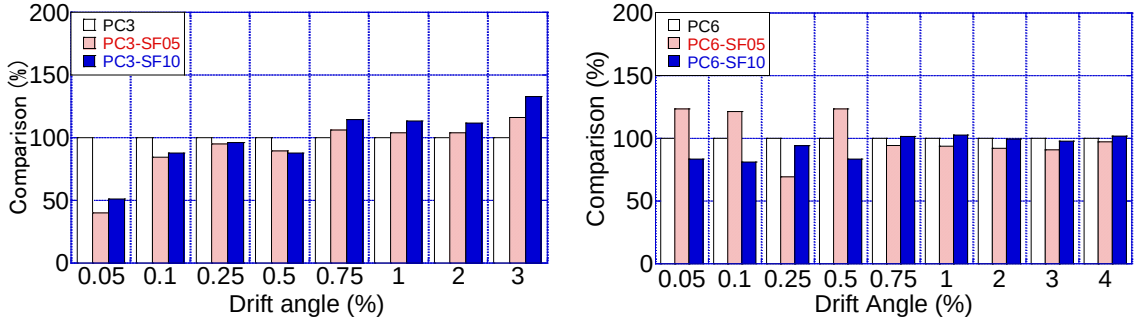

(a) PC3 series (b) PC6 series

Fig. 11 Comparison of energy dissipation capacity at second cycle

Fig. 11 shows the comparison results of energy dissipation capacity at second cycle for all specimens. PC3-SF05 and PC3-SF10 specimens dissipated more energy than PC3 from 0.5 percent drift angle. In addition, PC3-SF10 dissipated more energy than PC3-SF05 by difference of volume fraction of steel-fiber 0.5 percent.
On the other hand, for PC6 series, energy dissipation was almost similar as shown in **Fig. 11 (b)**. This is because the effect of PC strands was more important than the reinforcing effect by steel-fibers.

Ultimate Flexural Strength of PreSFC Member

Several empirically and analytically methods have been developed to predict the ultimate flexural strength of steel-fiber reinforced concrete members. Methods proposed by Swamy[5] and Hengaer[6] are examined. Swamy employed the theory of composite material and take into account a random distribution factor, bond stress, fiber stress and other factors. Swamy proposed the ultimate flexural strength calculation method of SFRC beams as given by Eq. (4)[5].

$$M_{sw,u}=F_c(d_n-k_2)+F_{sc}(d_n-d')+F_{st}(d-d_n)+F_{ft}(D-d_n)/2 \quad (4)$$

in which F_c: concrete compression force (N/mm^2), d_n: neutral axis depth (mm), k_2: depth of centroid compression block (mm), F_{sc}: force in compression reinforcement (kN), d': depth of compression reinforcement (mm), F_{st}: force in tension steel (kN), d: depth of tension steel (mm), F_{ft}: force in fibers in tension zone (kN).

Henager presented an analytical method to predict the flexural strength, in which the bond stress, fiber aspect ratio, and volume fraction of fibers were taken into account. Henager proposed Eq. (5) for the ultimate flexural strength calculation of SFRC[6].

$$M_{he,u}=A_s\cdot\sigma_y(d-a/2)+\sigma_t\cdot b(h-e)\cdot(h/2+e/2-a/2) \quad (5)$$

in which A_s: area of tensile mild steel (mm^2), σ_y: yield stress of steel (N/mm^2), d: effective depth of cross section (mm), a: depth of rectangular stress block (mm), e: distance from the extreme compression fiber to top of tensile stress block of fibrous concrete (mm).
In this research, in order to apply these equations to pretensioned members, terms considering PC strands contribution were included in Eq. (6) and (7).

$$M_{sw,u}=F_c(d_n-k_2)+F_{sc}(d_n-d')+F_{st}(d-d_n)+F_{ft}(D-d_n)/2+F_{py}(d_p-d_n) \quad (6)$$

$$M_{he,u}=A_s\cdot\sigma_y(d-a/2)+\sigma_t\cdot b(h-e)\cdot(h/2+e/2-a/2)+A_p\cdot\sigma_{py}(d_p-a/2)-A_p\cdot\sigma_{pc}(d'_p-a/2) \quad (7)$$

in which F_{pc}: force in compressive PC strand (kN), d'_p: depth of compressive PC strand (mm), F_{py}: force in tension PC strand (kN), d_p: depth of tension PC strand (mm), A_p: area of tensile PC strand (mm^2), σ_{py}: tensile stress of PC strand (N/mm^2), d_p: depth of tensile PC strand (mm), A_{pc}: area of compressive PC strand (mm^2), σ_{pc}: compressive stress of PC strand (N/mm^2), d'_p: depth of compressive PC strand (mm).

Table 11 summarizes the comparison results of all PreSFC members. In the table, $Q_{0.3}$ is the strength when the compressive concrete strain reached 0.3%. The proposal methods by Swamy and Henager are not related to the maximum strength of SFRC. They proposed the evaluation equation at concrete compressive strain corresponding to 0.3 percent (Swamy) and 0.35 (Henager) percent. The error ratio for PC3 series varied from

Table 11 Comparison of calculated ultimate flexural strengths and test results

Specimens	Test results	Swamy	Henager	$Q_{0.3}/Q_{sw}$	$Q_{0.3}/Q_{he}$
	$Q_{0.3}$ *1 (kN)	Q_{sw} *2 (kN)	Q_{he} *3 (kN)		
PC3-SF05	349.7	452.4	538.0	0.77	0.65
PC3-SF10	387.5	461.6	560.0	0.84	0.69
PC6-SF05	367.2	550.8	661.9	0.67	0.55
PC6-SF10	352.1	558.8	656.4	0.63	0.54

*1: the strength at reached the compressive concrete strain is 0.3%, *2: the strength by modified Swamy, Eq. (6), *3: the strength by modified Henager, Eq. (7)

0.65 to 0.84 by Eq. (6) and (7). In addition, PC6 series show the error ratio varying from 0.54 to 0.67. The proposed methods by Swamy and Henager are overestimating the reinforcing effect by steel-fiber at 0.3 percent concrete compressive strain. It was experimentally observed that the reinforcing effect by steel-fibers was not significant ultimate state.

CONCLUSIONS

Two traditional pretensioned beams (PC3, PC6) and four pretensioned beams using SFRC (PC3-SF05, PC3-SF10, PC6-SF05, PC6-SF10) were constructed and statically loaded to study the effect of SFRC on the seismic performance of pretensioned beams. The following conclusions were drawn from the results of this investigation.

1) The ultimate flexural strengths of all SF05 specimens (PC3-SF05, PC6-SF05) and SF10 specimens (PC3-SF10, PC6-SF10) were in average 9.3 and 6.4 percent larger than that of traditional pretensioned members (PC3 and PC6).

2) Specimen PC3 showed permanent damage since the cover concrete had spalled off and the prestressing strands and mild reinforcement were exposed. However, for PC3-SF05 and PC3-SF10, the concrete spalling did not occur. In addition, it can be seen for PC3-SF10 that the number of shear cracks was less than that for PC3 and PC3-SF05. However, PC6 specimen did not show cover concrete spalling like for PC3 specimen. Moreover, it can be seen for PC6-SF05 and PC6-SF10 that the number of shear cracks was less than that for PC6 and PC3 series specimens. This is because there was a shear reinforcing effect by steel-fiber reinforced concrete.

3) Energy dissipation capacities of PC3-SF05 and PC3-SF10 after 0.5% drift angle were 5 to 9 % and 10 to 14 % larger than that of PC3 because SFRC resulted in larger residual deformations for PC3-SF05 and PC3-SF10 than for PC3. However, PC6 series specimens dissipated almost the same energy. This was attributed to the effect of PC strands that was more important than the reinforcing effect by steel-fibers.

4) The proposed methods by Swamy and Henager overestimated the reinforcing effect by steel-fibers at 0.3 percent concrete compressive strain. The reinforcing effect by steel-fibers at the ultimate state was not significant.

ACKNOWLEDGMENT

This research was supported by JSPS KAKENHI Grant Number 24-5797.

REFERENCES

1. Minoru Kunieda, Keitetsu Rokugo, "Recent progress on HPFRCC in Japan", J*ournal of Advanced Concrete Technology*, *JCI*, Vol. 4, No.1, 19-33, 2006.
2. Haruhiko Suwada, Hiroshi Fukuyama, "Experimental and analytical study on influencing factors on shear strength and deformation capacity of damper using high performance fiber reinforced cementitious composite", *J. Struct. Constr. Eng.*, *AIJ*, No.612, 171-178, 2009. (in Japanese)
3. Haruhiko Suwada, Hiroshi Fukuyama, "Noliner finite element analysis on shear failure of structural elements using high performance fiber reinforced cement compsite", *Journal of Advanced Concrete Technology*, *JCI*, Vol. 4, No.1, 45-57, 2006.
4. Bilal S. Hamad, Mohamad H. Harajli, and Ghaida' Juma, "Effect of fiber reinforcement on bond strength of tension lap splices in high-strength concrete", *Structural Journal*, *ACI*, Vol. 78, No.36, 395-405, 2001.
5. R. N. Swamy, Sa'ad A. Al-Ta'an, "Deformation and ultimate strength in flexural of reinforced concrete beams made with steel fiber concrete", *Structural Journal*, *ACI*, Vol. 78, No.36, 395-405, 1981.
6. Charles H. Henager, M. ASCE and Terrance J. Doherty, "Analysis of reinforced fibrous concrete beams", *Journal of Structural Division*, *ASCE*, Vol. 102, No.ST1, 177-188, 1976.
7. Hyeong Jae YOON, Minehiro NISHIYAMA, "Behavior of Pretensioned Concrete Beams Using Steel-fiber Reinforced Concrete", 15th World Conference of Earthquake Engineering, Lisbon, Portugal, 2012.
8. S. K. Padmarajaiah and Ananth Ramaswamy, "Behavior of fiber-reinforced prestressed and reinforced high-strength concrete beams subjected to shear", *Structural Journal*, *ACI*, Vol. 98, No.5, 752-761, 2001.
9. Japan Architecture Center, *Design and calculation example of Prestressed Concrete Technical Standard*, 2009. (in Japanese)
10. Hyeong Jae YOON, "Seismic Performance of Prestressed Concrete Beams Using Steel-Fiber Reinforced Concrete", Ph.D. Thesis, Kyoro University, 2014.